

1 Host adaptation through hybridization: Genome analysis of triticale
2 powdery mildew reveals unique combination of lineage-specific effectors

3

4 Marion C. Müller, Lukas Kunz, Johannes Graf, Seraina Schudel, Beat Keller*

5

6 Department of Plant and Microbial Biology, University of Zurich, Zurich, Switzerland

7

8 * Corresponding author: Beat Keller, Email: bkeller@botinst.uzh.ch

9

10 Keywords: hybridization, powdery mildew, lineage specific effector, triticale

11

12

13 Funding: University Research Priority Program "Evolution in Action" of the University of Zürich Swiss
14 National Science Foundation grant 310030B_182833

15

16 **Abstract**

17 The emergence of new fungal pathogens through hybridization represents a serious challenge for agriculture.
18 Hybridization between the wheat mildew (*Blumeria graminis f.sp. tritici*) and rye mildew (*B.g. f.sp. secalis*)
19 pathogens have led to the emergence of a new mildew form (*B.g. f.sp. triticales*) growing on triticale, a man-made
20 amphiploid crop derived from crossing rye and wheat which was originally resistant to the powdery mildew
21 disease. The identification of the genetic basis of host-adaptation in triticale mildew has been hampered by the
22 lack of a reference genome. Here we report the 141.4 Mb reference assembly of *B.g. triticales* isolate THUN-12
23 derived from long-read sequencing and genetic map-based scaffolding. All eleven *B.g. triticales* chromosomes were
24 assembled from telomere-to-telomere and revealed that 19.7% of the hybrid genome was inherited from the rye
25 mildew parental lineage. We identified lineage-specific regions in the hybrid, inherited from the rye or wheat
26 mildew parental lineages, that harbour numerous bona fide candidate effectors. We propose that the combination
27 of lineage-specific effectors in the hybrid genome is crucial for host-adaptation, allowing the fungus to
28 simultaneously circumvent the immune systems contributed by wheat and rye in the triticale crop. In line with this
29 we demonstrate the functional transfer of the *SvrPm3* effector from wheat to triticale mildew, a virulence effector
30 that specifically suppresses resistance of the wheat *Pm3* allelic series. This transfer is the likely underlying cause
31 for the observed poor effectiveness of several *Pm3* alleles against triticale mildew and exemplifies the negative
32 implications of pathogen hybridizations on resistance breeding.

33

34 **Main Text**

35 The emergence of new fungal pathogens on crops poses a serious problem for agriculture. One mechanism by
36 which fungal pathogens can adapt to a new host is hybridization, by which two different pathogen lineages
37 recombine their gene complement enabling them to infect a new host species (Thines, 2019). Despite several
38 reports of hybridizations in plant pathogens, host adaptation by hybridization is poorly understood and the genetic
39 loci involved remain unidentified (reviewed in (Stukenbrock, 2016).

40 A prominent example of a host-adaptation through hybridization is the recent emergence of the triticale powdery
41 mildew (*Blumeria graminis f.sp. triticales*) on the cereal crop triticale in the year 2001 (Walker *et al.*, 2011). *B.g.*
42 *triticales* was found to be the result of hybridization events between the highly host-specific fungal sub-lineages of
43 wheat (*B.g. tritici*) and rye (*B.g. secalis*) powdery mildew (Menardo *et al.*, 2016). The hybridization on the
44 pathogen side mirrored the breeding history of its new host, which is an amphiploid resulting from a cross of the
45 two cereal crops wheat (*Triticum. sp.*) and rye (*Secale cereale*) (Oettler, 2005). Triticale has seen an increase in
46 cultivation in the past decades especially in Europe (Arseniuk, 2014). Unfortunately, disease outbreaks of powdery
47 mildew on triticale have increased both in number and severity and corroborates the need for resistance breeding
48 in this crop (Mascher *et al.*, 2006; Kowalczyk *et al.*, 2011; Arseniuk, 2014).

49 Previous analyses of the triticale powdery mildew hybrid pathogen were based on the wheat mildew reference
50 genome (Menardo *et al.*, 2016; Praz *et al.*, 2018). This approach suffers from its bias to the gene content of one of
51 the parental lineages of the hybrid. This is particularly relevant since effectors, small, secreted proteins that are
52 encoded by hundreds of genes in powdery mildew genomes, reside in highly dynamic gene clusters that often
53 show copy number variation or lineage specific expansions (Menardo *et al.*, 2017; Frantzeskakis *et al.*, 2018;
54 Müller *et al.*, 2019). Due to their dual role in infection as putative virulence factors suppressing the host defences
55 as well as avirulence factors recognised by major resistance genes, effector genes represent prime candidates for
56 host-specificity factors (Li *et al.*, 2020). In this study we present a chromosome-scale assembly of triticale powdery
57 mildew that will lay the foundation to understand host adaptation through hybridization in the cereal powdery
58 mildew pathosystem.

59

60 We sequenced *B.g. triticale* isolate THUN-12 using PacBio technology to a sequencing depth of 180X to establish
61 a reference assembly of the hybrid powdery mildew. The resulting assembly was 141.1 Mb in size and consisted
62 of 51 contigs. We used the previously described scaffolding method based on the genetic map of the fully
63 sequenced mapping population of THUN-12 X *B.g. tritici* Bgt_96224 (Müller *et al.*, 2019) to scaffold the contigs
64 into eleven chromosomes (Table S1). Three of the eleven chromosomes, namely Chr-03, Chr-06 and Chr-10, were
65 assembled in a single contig in the THUN-12 assembly. The remaining chromosomes were scaffolded with a
66 maximum of three scaffold gaps. In addition, the genetic map allowed to correct three assembly errors, in which
67 chromosomes arms originating from different chromosomes were fused in the centromeric regions. With a
68 transposable element content of 69.4%, the *B.g. triticale* genome exhibits a characteristic genome organization
69 with high repeat content, reminiscent of other sequenced *B. graminis* isolates. (Frantzeskakis *et al.*, 2018; Müller
70 *et al.*, 2019) We found a single region per chromosome with a distinct transposable element content consisting of
71 non-long-terminal-repeat retrotransposons, corresponding to the genetic centromere (Figure S1). In addition, we
72 found stretches of telomeric repeats TAACCC at all ends of the eleven chromosomes (Figure S1). The presence
73 of telomeres and the centromere on each chromosome together with the low number of scaffold gaps indicates
74 high completeness of all eleven chromosomes resolved in the *B.g. triticale* assembly. This represents a significant
75 improvement to previous high-quality assemblies of the *Blumeria graminis* species, which still contain hundreds
76 of gaps or unresolved chromosomal regions (Frantzeskakis *et al.*, 2018; Müller *et al.*, 2019).

77 The high-quality genome of THUN-12 allowed us to study the signature of hybridization between *B.g. tritici* and
78 *B.g. secalis* at the chromosomal level. As described in (Menardo *et al.*, 2016) we used fixed polymorphisms
79 between *B.g. secalis* and *B.g. tritici* to attribute genomic segments in THUN-12 to the two parental sub-lineages
80 ((Menardo *et al.*, 2016). We found that 80.3% of the THUN-12 genome is inherited from wheat mildew and 19.7%
81 was inherited from rye mildew (Figure 1, Table S1). The observed higher percentage of segments with wheat
82 mildew origin in the THUN-12 isolate is consistent with the previously proposed scenario in which the first
83 rye/wheat mildew hybrids backcrossed to wheat mildew after the initial hybridization (Menardo *et al.*, 2016).
84 During meiosis, at least one crossover takes place between homologous chromosomes (Marston & Amon, 2004).
85 Indeed, we found at least one recombination event between wheat and rye mildew per chromosome, suggesting
86 efficient chromosomal pairing in all chromosomes between the two parental lineages during the initial
87 hybridization. Strikingly, the size of segments inherited from *B.g. secalis* varied considerably and proportional
88 contribution to chromosomes ranged from 6.0% on Chr-09 to a maximum of 40.9% on Chr-04 (Figure 1, Table
89 S1). In addition, the location of the *B.g. secalis* segments is highly variable between chromosomes, for instance,
90 eight of the eleven chromosomes inherited at least one telomeric sequence from *B.g. secalis*. In contrast, Chr-07

91 contains a single, larger segment inherited from *B.g. secalis* that overlaps with the genetic centromere. The
92 centromeres of all other chromosomes were inherited from *B.g. tritici*. To what degree the differential proportion
93 of *B.g. secalis* segments per chromosome are the result of differential contribution to host-adaptation or purely
94 stochastic based on the limited amount of recombination between the parental strains remains to be determined in
95 further studies.

96 The availability of the hybrid THUN-12 genome and the previously published chromosome-scale assembly of the
97 wheat mildew Bgt_96224 (Müller et al., 2019) allowed the comparison of the hybrid genome to the wheat mildew
98 parental lineage.. Upon whole-genome alignment of the two genomes (Figure S3) using the MUMmer software
99 (Kurtz *et al.*, 2004) 99.26% of the THUN-12 genome was aligned to the Bgt_96224 genome. We observed a high
100 co-linearity across the eleven chromosomes in *B.g. tritici* inherited regions as well as in the 27.7 Mb of sequence
101 originating from *B. g. secalis* (Figure S3). The analysis identified only a few (<20) regions with major
102 rearrangements, most of which overlap with the genetic centromeres and likely represent assembly artefacts
103 (Figure S3). The centromeres consist exclusively of repetitive elements and are therefore often not completely
104 resolved despite the long-read sequencing technology (Müller et al. 2019). In addition, we identified a large
105 inversion on Chr-02. The inverted region in Bgt_96224 is however flanked by sequence gaps and could therefore
106 be explained by a scaffolding error in the Bgt_96224 assembly. The most interesting major difference between the
107 genomes is a telomeric region of Chr-11 which is absent in the assembly of Bgt_96224 (Figure S2) and therefore
108 represents a candidate lineage-specific region in THUN-12 which was inherited from *B.g. secalis* (see below).
109 When we considered smaller rearrangements (>1kb, <10kb) predicted by the MUMmer software, we found
110 evidence for alignment breaks that constitute inversions, gaps and duplications on all chromosome (Table S4).
111 Segments inherited from *B.g. secalis* were significantly enriched for such rearrangements compared to segments
112 inherited from *B.g. tritici*, which is consistent with the divergence of the two fungal lineages ca. 160'000-250'000
113 ya (Table S4, (Menardo *et al.*, 2016). Due to the predominance of small-scale rearrangements identified by
114 comparison to *B.g. tritici*, we concluded that the two parental f.sp. of the hybrid have a very similar overall genome
115 structure. This is consistent with our findings in the experimental population Bgt_96224 X THUN-12 for which
116 we found no impairment of recombination in segments inherited from *B. g. secalis*. (Müller et al. 2019). We
117 therefore propose that the high similarity of the two genomes provided the basis for the successful hybridization
118 of *B.g. secalis* and *B.g. tritici* that gave rise to the first *B.g. triticales* hybrids and that the occurrence of hybridization
119 of these lineages was mainly limited by suitable host plants in the past.

120 The process of hybridization allows the combination of genes or genomic regions that are normally present only
121 in one particular fungal lineage, but absent in the other. In numerous fungal plant pathogens host-adaptation has
122 been attributed to the occurrence of lineage-specific effector proteins acting as virulence factors (i.e. allowing
123 growth on the particular host) or avirulence factors (i.e. preventing growth due to recognition by host specific
124 immune receptors). To identify putative effector genes in the *B.g. triticales* hybrid, we performed a de-novo gene
125 annotation based on the previously published proteins of *B.g. tritici* and *B.g. hordei*. This resulted in the annotation
126 of 7,993 genes including 1,011 candidate effectors that were subsequently assigned to the previously described
127 *Blumeria* candidate effector families (Müller *et al.*, 2019). To test for the parental contribution to the gene content
128 of the hybrid we determined for each gene whether it is encoded in a segment derived from wheat or rye mildew.
129 We found that a total of 20 % of all genes in THUN-12 were encoded within a segment of *B.g. secalis*. To define
130 lineage-specific effectors we used genomic coverage based on resequencing data from *B.g. tritici* or *B.g. secalis*
131 isolate to predict the absence of the THUN-12 candidate effectors in all isolates within one parental forma specialis
132 (Note S2). We identified five loci containing candidate, lineage-specific effector genes inherited from *B.g secalis*
133 in the telomeric regions of Chr-01, Chr-04, and Chr-11 and on the chromosome arms of Chr-08 and Chr-09 (Figure
134 1). Upon comparison with the Bgt_96224 genome, we could confirm the absence of these effector genes within
135 the wheat mildew lineage (Figure 2, Note S3). For instance, the *B.g. secalis* lineage-specific region on Chr-01 in
136 THUN-12 contains a three-fold tandem duplication of two effectors belonging to family E135 and E001,
137 respectively, whereas the corresponding region in Bgt_96224 contains only one gene each (Figures 2A, S6B). On
138 Chr-04 we found a cluster of the E029 effector family with 9 members in THUN-12 and 6 members in Bgt_96224.
139 Therefore, this cluster predates the split between *B.g. secalis* and *B.g. tritici*, but rearrangements within the cluster
140 have led to three lineage-specific effectors in *B.g. secalis* (Figure 2B). The third example represents the above-
141 mentioned lineage-specific region on THUN-12 Chr-11 which was found to be partially absent from the
142 Bgt_96224 assembly. The region contains six candidate effector genes of which three belong to family E003 and
143 are lineage-specific for *B.g secalis* (Figure 2C). The remaining two regions on Chr-08 and Chr-09 contained a
144 single effector gene present in THUN-12 but absent from Bgt_96224 belonging to E004 and E001, respectively
145 (Figure 2D,E). It is worth noting that several of the identified *B.g. secalis* lineage-specific candidates exhibit
146 similarities with validated virulence or avirulence factors in *B.g. tritici* and *B.g. hordei* (Note S4). For example,
147 several candidates belong to a group of small, highly expressed candidate effector families (termed group 1
148 effectors) harboring most of the virulence/avirulence factors in the *Blumeria* genus identified to date (Müller *et*
149 *al.*, 2019). Similarly, numerous genes are predicted to exhibit structural similarities (RNase-like fold) to cloned
150 avirulence genes and virulence factors (Figure S5) (Bauer *et al.*, 2021). Most importantly, several lineage-specific

151 candidates exhibit very high expression levels during the crucial phase of haustoria establishment (Figure S5), a
152 hallmark of avirulence factors in wheat mildew (Bourras *et al.*, 2019).

153 Using the same coverage-based approach we also identified several regions containing candidate effector genes
154 absent from the *B.g. secalis* lineage. We found four loci with strong signatures of *B.g. tritici* lineage-specificity on
155 Chr-01, Chr-06 and Chr-11 (Figure 1). Strikingly, three loci overlapped with the known *B.g. tritici* gene clusters
156 harbouring *AvrPm17* (Chr-01), *AvrPm3^{a2/f2}* (Chr-06) and *AvrPm1a* (Chr-06) (Note S5). It was previously
157 hypothesized that the strong selection pressure exerted by corresponding resistance genes in wheat has led to
158 effector cluster expansions in these regions in the *B.g. tritici* lineage (Müller *et al.*, 2019; Hewitt *et al.*, 2020;
159 Müller *et al.*, 2021). The fourth region showing a high density of *B.g. tritici* specific effectors on Chr-11 of THUN-
160 12 might consequently harbour a so far unidentified avirulence gene. Interestingly the *B.g. tritici* lineage-specific
161 effectors on Chr-11 belong to the E003 family. Gene members of the same family are also present in the *B.g. tritici*
162 specific locus on Chr-01 (*AvrPm17*, (Müller *et al.*, 2021)) and the *B.g. secalis* specific region on the other arm of
163 Chr-11 (see above). The E003 family members therefore represent prime candidates for effectors involved in host-
164 adaptation on triticale. In summary we found that the *B.g. triticales* hybrid contains lineage-specific effectors
165 inherited from both parental lineages. We hypothesize that these regions play a role in host-adaptation and
166 virulence of triticale powdery mildew on the new host triticale, enabling the fungus to cope with both the rye and
167 wheat immune system, simultaneously present in triticale.

168 As described above, three loci with strong evidence for a lineage-specific expansion in THUN-12 correspond to
169 the previously identified *AvrPm1a*, *AvrPm17* and *AvrPm3^{a2/f2}* loci in wheat mildew. In addition, the regions
170 corresponding to the other cloned wheat mildew avirulence genes, namely *AvrPm2*, *AvrPm3^{b2/c}*, *AvrPm3^{d3}* are also
171 encoded in segments from wheat mildew in THUN-12. Therefore, the genomes of THUN-12 and Bgt_96224
172 provided us with a unique opportunity to compare all the previously described wheat mildew avirulence loci in
173 two high quality genomes (Figure 3A-F). This comparison allowed us to confirm previous observations based on
174 short read-sequencing data. For instance, THUN-12 contains three *AvrPm3^{a2/f2}* genes, as we have previously
175 predicted for many *B.g. tritici* isolates based on genomic coverage (Müller *et al.*, 2019). Furthermore, the
176 *AvrPm3^{b2/c2}*-locus contains an additional candidate effector in THUN-12 that is pseudogenized in Bgt_96224 by a
177 transposable element insertion (Bourras *et al.*, 2019), whereas the *AvrPm3^{d3}*-locus exhibits several small scale
178 insertions surrounding the avirulence gene. Also, THUN-12 contains the known deletion covering the *AvrPm2*
179 gene, a deletion that is adaptive since it allows mildew to overcome *Pm2* mediated resistance in wheat (Praz *et al.*,
180 2017). In addition, we could detect new variation previously undetected such as a small inversion affecting an

181 effector in the *AvrPm1a* locus as well as a non-allelic gene conversion event in the newly identified *AvrPm17*
182 paralogous effector pair (see (Müller *et al.*, 2021). Strikingly, despite the dynamic nature of these avirulence loci,
183 the THUN-12 isolate, with the exception of the deleted *AvrPm2*, encodes for the avirulent allele of all five
184 avirulence genes. It was previously proposed that avirulence genes in powdery mildew exert an important virulence
185 function on wheat (McNally *et al.*, 2018; Bourras *et al.*, 2019). We therefore hypothesize that the functional
186 conservation of *B.g. tritici* avirulence effectors in *B.g. triticales* provides the hybrid pathogen with increased
187 virulence capacity, at least in the absence of corresponding resistance genes in triticale.

188 To test the functionality of the *B.g. tritici* avirulence genes in the hybrid genetic background, we analysed their
189 expression during early infection on triticale at the timepoint of haustorium formation (i.e. 48hpi). Similar to the
190 situation in wheat mildew, the avirulence genes are consistently among the highest expressed genes in THUN-12
191 (Figure 4A, Müller *et al.*, 2021). In line with this, THUN-12 is avirulent on wheat lines containing *Pm1a*, *Pm17*,
192 *Pm3a*, *Pm3b* and *Pm3d* (Figure 4B). We however observed virulent phenotypes of THUN-12 on near isogenic
193 lines (NILs) containing *Pm3f* (weak allele of *Pm3a*) and *Pm3c* (weak allele of *Pm3b*), despite the presence of
194 *AvrPm3^{a2/f2}* and *AvrPm3^{b2/c2}* (Figure 4B). To resolve this phenotypic/genotypic discrepancy, we performed QTL
195 mapping based on 55 progeny of the Bgt_96224 X THUN-12 population on the *Pm3c*-containing wheat line
196 Sonora/8*CC. We found a single QTL (LOD=9.44) on Chr-04 (Figure 4C) that corresponds to the previously
197 described *SvrPm3*-locus in wheat mildew (Bourras *et al.*, 2015; Parlange *et al.*, 2015). *SvrPm3* encodes an effector
198 that suppresses resistance mediated by *Pm3a -f*. Indeed, THUN-12 contains the active *SvrPm3* haplovariant, again
199 encoded by a wheat mildew segment (Figures 1,4D, S6), whereas Bgt_96224 encodes the inactive allele (Bourras
200 *et al.*, 2015; Parlange *et al.*, 2015). Thus, the virulent phenotype of THUN-12 on the weak *Pm3c* and *Pm3f* alleles
201 (Brunner *et al.*, 2010) can be explained by the presence of the *SvrPm3* suppressor gene, efficiently masking
202 recognition of *AvrPm3^{a2/f2}* and *AvrPm3^{b2/c2}*, thereby demonstrating the functionality of a major wheat mildew
203 virulence factor in the hybrid genetic background. Since *B.g. secalis* encodes for an inactive *SvrPm3* haplovariant
204 (Bourras *et al.*, 2019), the active variant could only be inherited from the *B.g. tritici*. The presence of the active
205 *SvrPm3* in the triticale mildew population likely has implications for triticale breeding. It was previously
206 demonstrated that *SvrPm3*-based suppression is quantitative and that isolates expressing the *SvrPm3* to very high
207 levels are able suppress also the stronger *Pm3a* and *Pm3b* alleles (Bourras *et al.*, 2015; Bourras *et al.*, 2019).
208 Therefore, the presence of *SvrPm3* in the *B.g. triticales* population potentially renders the entire *Pm3*-allelic series
209 ineffective for controlling mildew on triticale. Indeed, previous studies have found virulence proportion of over
210 40% towards several *Pm3*-alleles in the triticale powdery mildew population of Poland, France and Belgium

211 (Czembor *et al.*, 2013; Troch *et al.*, 2013; Czembor *et al.*, 2014). We propose that these results can be explained
212 by the presence of the active *SvrPm3* in these populations.

213 In summary, we present a chromosome-scale genome assembly of the *B.g. triticales* hybrid pathogen based on
214 significant advances in long-read sequencing technology and a high-resolution genetic map thereby allowing a
215 molecular analysis of the hybrid genome structure of a fungal plant pathogen. The *B.g. triticales* genome is defined
216 as a mosaic between two highly collinear parental genomes of wheat and rye powdery mildew and includes several
217 lineage specific regions harbouring highly expressed candidate effector genes. The reference genome of *B.g.*
218 *triticales* provides the basis for future identification and functional validation of virulence factors involved in host-
219 adaptation on triticales. We furthermore provide evidence that avirulence and suppressor genes identified in wheat
220 mildew are fully functional in *B.g. triticales* and thereby exemplify the importance of genomic analyses of plant
221 pathogens for resistance breeding in triticales. We propose to pre-emptively combine genomic resources and
222 pathogen diversity analyses to increase the efficiency of resistance breeding in triticales and beyond.

223

224

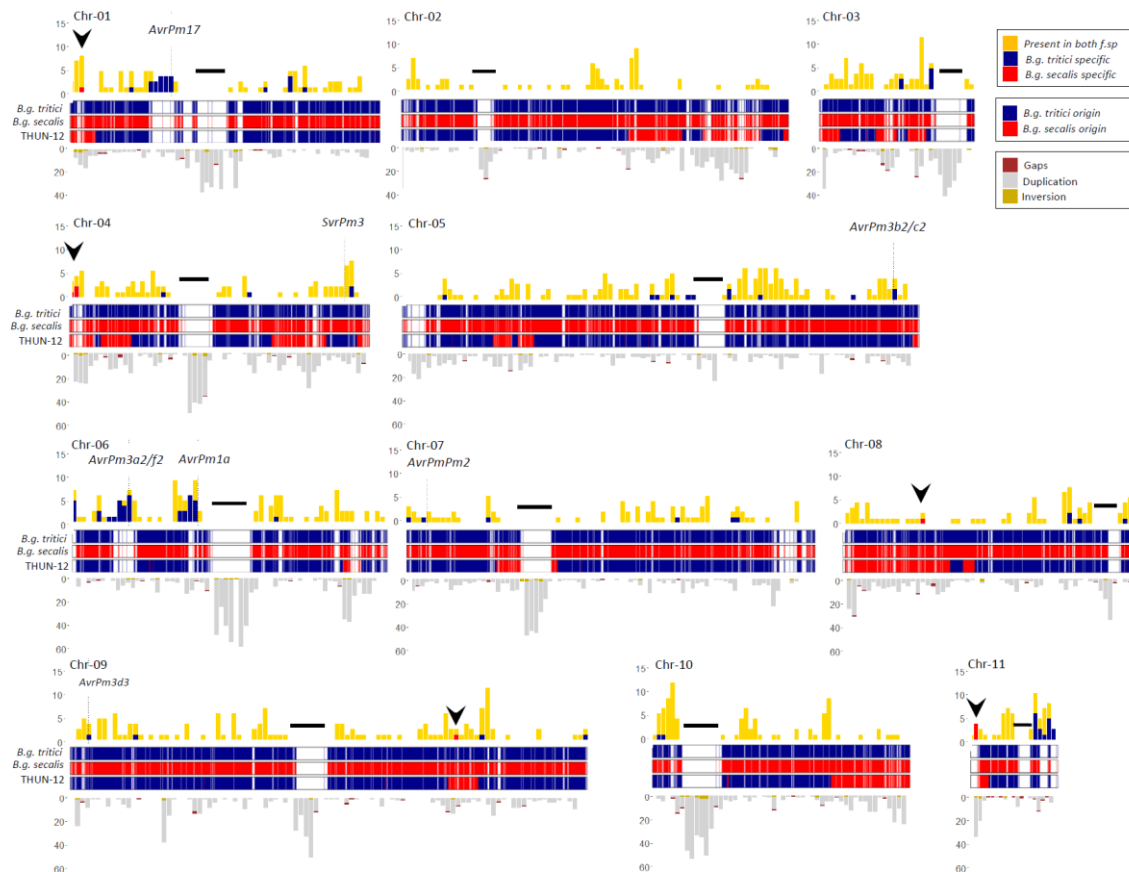
225 References

- 226 **Arseniuk E. 2014.** Triticale biotic stresses--an overview. *Communications in agricultural and applied*
227 *biological sciences* **79**(4): 82-100.
- 228 **Bauer S, Yu D, Lawson AW, Saur IML, Frantzeskakis L, Kracher B, Logemann E, Chai J, Maekawa T,**
229 **Schulze-Lefert P. 2021.** The leucine-rich repeats in allelic barley MLA immune receptors
230 define specificity towards sequence-unrelated powdery mildew avirulence effectors with a
231 predicted common RNase-like fold. *PLoS pathogens* **17**(2): e1009223-e1009223.
- 232 **Bourras S, Kunz L, Xue MF, Praz CR, Muller MC, Kalin C, Schlafli M, Ackermann P, Fluckiger S,**
233 **Parlange F, et al. 2019.** The AvrPm3-Pm3 effector-NLR interactions control both race-specific
234 resistance and host-specificity of cereal mildews on wheat. *Nature Communications* **10**(1):
235 2292.
- 236 **Bourras S, McNally KE, Ben-David R, Parlange F, Roffler S, Praz CR, Oberhaensli S, Menardo F,**
237 **Stirnweis D, Frenkel Z, et al. 2015.** Multiple Avirulence Loci and Allele-Specific Effector
238 Recognition Control the Pm3 Race-Specific Resistance of Wheat to Powdery Mildew. *Plant*
239 *Cell* **27**(10): 2991-3012.
- 240 **Brunner S, Hurni S, Streckeisen P, Mayr G, Albrecht M, Yahiaoui N, Keller B. 2010.** Intragenic allele
241 pyramiding combines different specificities of wheat Pm3 resistance alleles. *Plant Journal*
242 **64**(3): 433-445.
- 243 **Czembor H, Doraczyńska O, Czembor J. 2013.** Resistance of triticale cultivars to powdery mildew (*Blu-*
244 *meria graminis* ff. ssp.) occurring in Poland. *Biul IHAR*(267): 3 – 16.
- 245 **Czembor HJ, Domeradzka O, Czembor JH, Mankowski DR. 2014.** Virulence Structure of the Powdery
246 Mildew (*Blumeria graminis*) Population Occurring on Triticale (x Triticosecale) in Poland.
247 *Journal of Phytopathology* **162**(7-8): 499-512.
- 248 **Frantzeskakis L, Kracher B, Kusch S, Yoshikawa-Maekawa M, Bauer S, Pedersen C, Spanu PD,**
249 **Maekawa T, Schulze-Lefert P, Panstruga R. 2018.** Signatures of host specialization and a
250 recent transposable element burst in the dynamic one-speed genome of the fungal barley
251 powdery mildew pathogen. *Bmc Genomics* **19**.
- 252 **Hewitt T, Mueller MC, Molnár I, Mascher M, Holušová K, Šimková H, Kunz L, Zhang J, Li J, Bhatt D,**
253 **et al. 2020.** A highly differentiated region of wheat chromosome 7AL encodes a Pm1a
254 immune receptor that recognises its corresponding AvrPm1a effector from *Blumeria*
255 *graminis*. *New Phytologist* n/a(n/a).
- 256 **Kowalczyk K, Gruszecka D, Nowak M, Lesniowska-Nowak J. 2011.** RESISTANCE OF TRITICALE
257 HYBRIDS WITH Pm4b AND Pm6 GENES TO POWDERY MILDEW. *Acta Biologica Cracoviensia*
258 *Series Botanica* **53**(1): 57-62.
- 259 **Kurtz S, Phillippy A, Delcher AL, Smoot M, Shumway M, Antonescu C, Salzberg SL. 2004.** Versatile
260 and open software for comparing large genomes. *Genome Biology* **5**(2).
- 261 **Li J, Cornelissen B, Rep M. 2020.** Host-specificity factors in plant pathogenic fungi. *Fungal genetics*
262 *and biology : FG & B* **144**: 103447-103447.
- 263 **Marston AL, Amon A. 2004.** Meiosis: Cell-cycle controls shuffle and deal. *Nature Reviews Molecular*
264 *Cell Biology* **5**(12): 983-997.
- 265 **Mascher F, Reichmann P, Schori A. 2006.** Einfluss des Mehltaus auf den Triticaleanbau. *AGRAR*
266 *Forschung* **13**(11-12): 500-504,.
- 267 **McNally KE, Menardo F, Luthi L, Praz CR, Muller MC, Kunz L, Ben-David R, Chandrasekhar K, Dinoor**
268 **A, Cowger C, et al. 2018.** Distinct domains of the AVRPM3(A2/F2) avirulence protein from
269 wheat powdery mildew are involved in immune receptor recognition and putative effector
270 function. *New Phytologist* **218**(2): 681-695.
- 271 **Menardo F, Praz CR, Wicker T, Keller B. 2017.** Rapid turnover of effectors in grass powdery mildew
272 (*Blumeria graminis*). *Bmc Evolutionary Biology* **17**: 223.
- 273 **Menardo F, Praz CR, Wyder S, Ben-David R, Bourras S, Matsumae H, McNally KE, Parlange F, Riba A,**
274 **Roffler S, et al. 2016.** Hybridization of powdery mildew strains gives rise to pathogens on
275 novel agricultural crop species. *Nature Genetics* **48**(2): 201-205.

- 276 **Müller MC, Kunz L, Schudel S, Kammerecker S, Isaksson J, Wyler M, Graf J, Sotiropoulos AG, Praz**
277 **CR, Wicker T, et al. 2021.** Standing genetic variation of the AvrPm17 avirulence gene in
278 powdery mildew limits the effectiveness of an introgressed rye resistance gene in wheat.
279 *bioRxiv*: 2021.2003.2009.433749.
- 280 **Müller MC, Praz CR, Sotiropoulos AG, Menardo F, Kunz L, Schudel S, Oberhänsli S, Poretti M,**
281 **Wehrli A, Bourras S, et al. 2019.** A chromosome-scale genome assembly reveals a highly
282 dynamic effector repertoire of wheat powdery mildew. *New Phytologist* **221**(4): 2176-2189.
- 283 **Oettler G. 2005.** The fortune of a botanical curiosity - Triticale: past, present and future. *Journal of*
284 *Agricultural Science* **143**: 329-346.
- 285 **Parlange F, Roffler S, Menardo F, Ben-David R, Bourras S, McNally KE, Oberhaensli S, Stirnweis D,**
286 **Buchmann G, Wicker T, et al. 2015.** Genetic and molecular characterization of a locus
287 involved in avirulence of *Blumeria graminis* f. sp. tritici on wheat Pm3 resistance alleles.
288 *Fungal Genetics and Biology* **82**: 181-192.
- 289 **Praz CR, Bourras S, Zeng FS, Sanchez-Martin J, Menardo F, Xue MF, Yang LJ, Roffler S, Boni R,**
290 **Herren G, et al. 2017.** AvrPm2 encodes an RNase-like avirulence effector which is conserved
291 in the two different specialized forms of wheat and rye powdery mildew fungus. *New*
292 *Phytologist* **213**(3): 1301-1314.
- 293 **Praz CR, Menardo F, Robinson MD, Müller MC, Wicker T, Bourras S, Keller B. 2018.** Non-parent of
294 Origin Expression of Numerous Effector Genes Indicates a Role of Gene Regulation in Host
295 Adaption of the Hybrid Triticale Powdery Mildew Pathogen. *Frontiers in Plant Science* **9**: 49.
- 296 **Stukenbrock EH. 2016.** The Role of Hybridization in the Evolution and Emergence of New Fungal
297 Plant Pathogens. *Phytopathology* **106**(2): 104-112.
- 298 **Thines M. 2019.** An evolutionary framework for host shifts - jumping ships for survival. *New*
299 *Phytologist* **224**(2): 605-617.
- 300 **Troch V, Audenaert K, Vanheule A, Bekaert B, Hofte M, Haesaert G. 2013.** Evaluation of Resistance
301 to Powdery Mildew in Triticale Seedlings and Adult Plants. *Plant Disease* **97**(3): 410-417.
- 302 **Walker AS, Bouguennec A, Confais J, Morgant G, Leroux P. 2011.** Evidence of host-range expansion
303 from new powdery mildew (*Blumeria graminis*) infections of triticale (xTriticosecale) in
304 France. *Plant Pathology* **60**(2): 207-220.

305

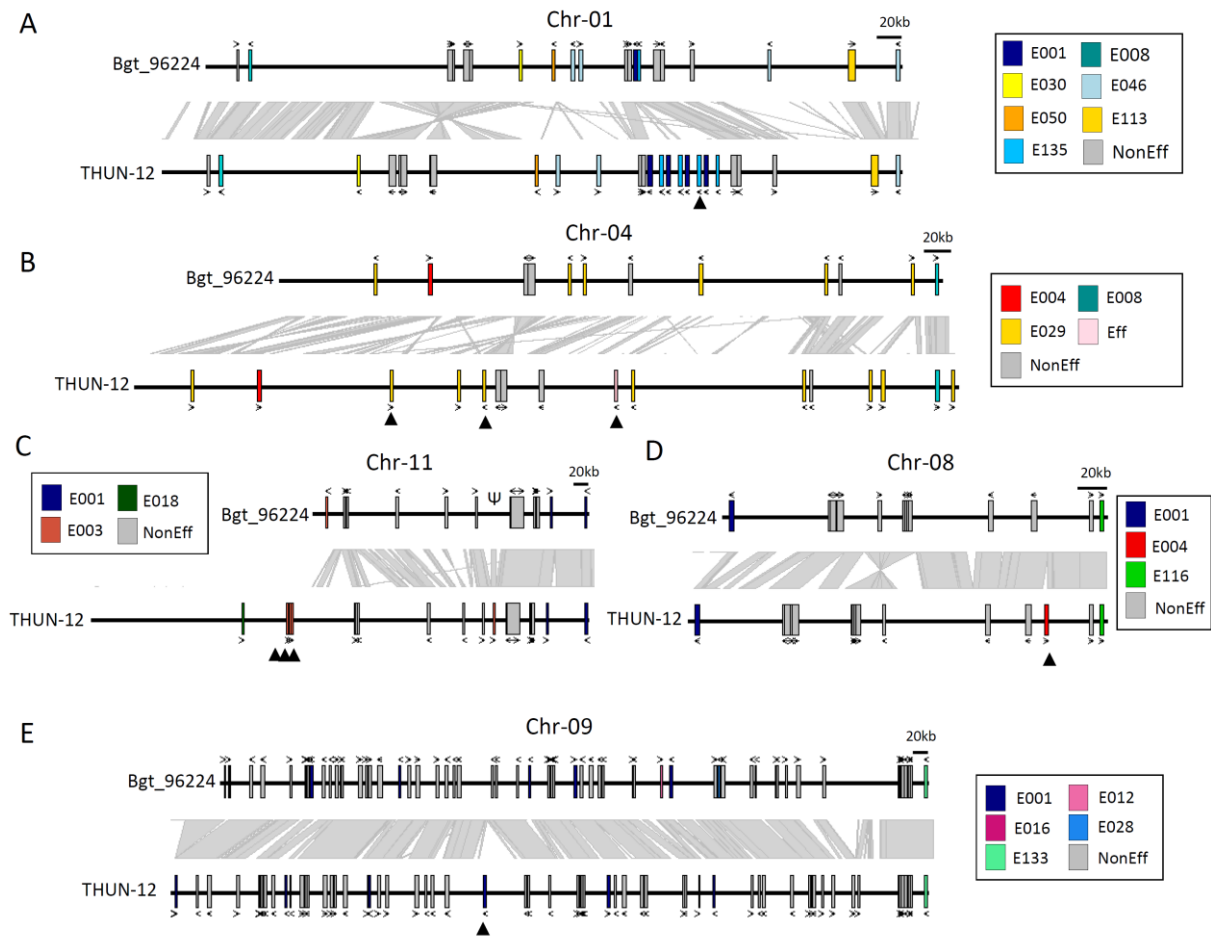
306



307

308 **Fig. 1 Overview of the eleven chromosomes of *B.g. triticales* THUN-12.** The first track shows the
309 distribution of candidate effector genes along the eleven chromosomes. Candidate effectors present in
310 both parental species *f.sp. tritici* and *f.sp. secalis* are indicated in yellow; candidate, lineage-specific
311 effector genes of *B.g. secalis* isolates are indicated in red and candidate, lineage-specific effector genes
312 of *B.g. tritici* are indicated in blue. Black arrowheads indicate the position of regions depicted in Figure
313 2. The second track indicates the genomic origin of the THUN-12 sequence, based on fixed
314 polymorphisms between *B.g. secalis* and *B.g. tritici*. SNPs originating from *B.g. secalis* are indicated in
315 red, SNPs originating from *B.g. tritici* are represented in blue. For each chromosome the position of the
316 genetic centromere is indicated by a black bar. The third track indicates number of putative alignment
317 breaks between *B.g. triticales* THUN-12 and *B.g. tritici* Bgt_96224 based on whole genome alignment
318 of the chromosome-scale assemblies of the two *f.sp.* by the MUMmer software. Putative rearrangements
319 were filtered and only rearrangements bigger than 1kb and smaller than 10kb are depicted. The
320 alignment breaks were depicted according to the prediction of the MUMmer software as follows: brown
321 indicates putative gaps, grey putative duplications and yellow indicates putative inversions.

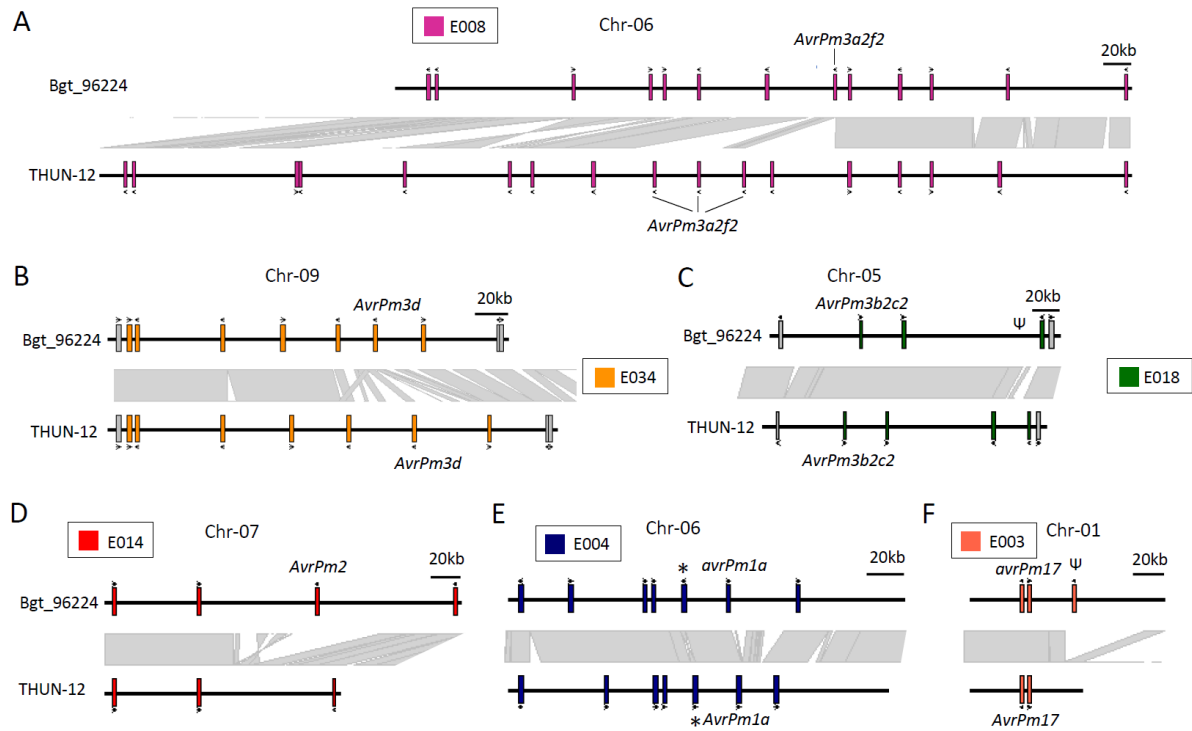
322



323

324 **Fig. 2 Identification of lineage-specific candidate effector genes in THUN-12 inherited from the *B.g. secalis***
325 **parental isolate. A-E)** Candidate effectors genes are indicated by colored boxes according to their candidate
326 effector family (Müller et al. 2019). Non-effector genes representing single copy orthologs determined by the
327 OrthoFinder software are indicated by grey boxes. In panel **B)**, Eff indicates an effector gene not assigned to a
328 candidate effector family. Gene direction is indicated above or below the gene. Co-linearity as determined by the
329 MUMmer software is indicated by grey rectangles between the gene tracks. Genes for which a lineage-specific
330 signal was detected are marked by a black arrowhead. **A-C)** represent the telomeric ends of Chr-01 **A)**, Chr-04 **B)**
331 and Chr-11 **C)**, whereas **D-E)** represent genomic loci within the chromosome arms of Chr-08 **D)** and Chr-09 **E)**.
332 The full description on the identification of the lineage-specific candidate effector is available in Note S3.

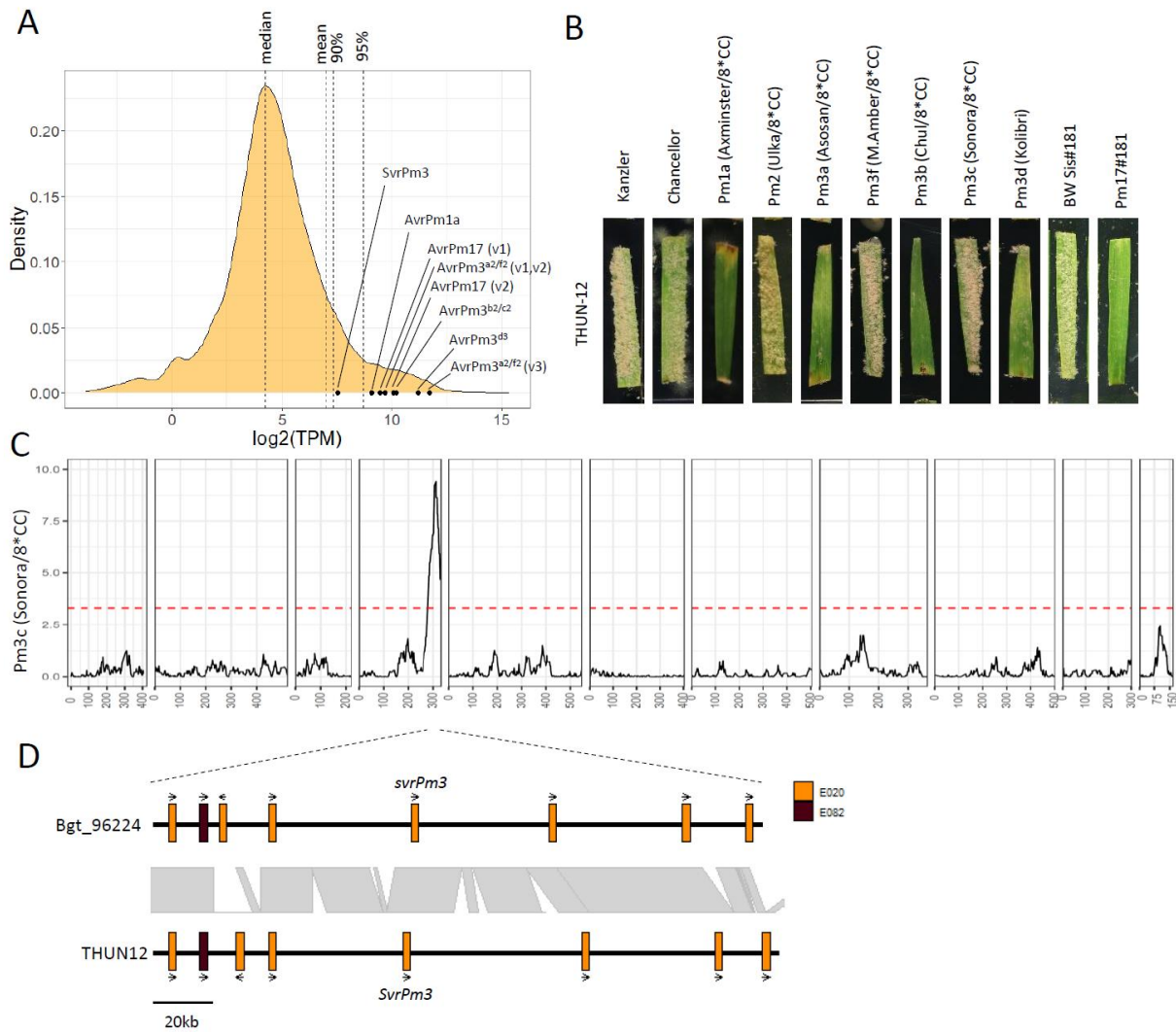
333



334

335 **Fig. 3 Comparison of six avirulence loci identified in wheat mildew between the *B.g. triticales* isolate THUN-**
336 ***12* and *B.g. tritici* isolate Bgt_96224. A-F) The hybrid mildew THUN-12 inherited all these loci from the *B.g.***
337 ***tritici* parental lineage. Genes are indicated by a box, gene orientation is indicated above or beneath the box.**
338 **Genome aligned as determined by the MUMmer software is indicated by grey rectangles between the gene tracks.**
339 **Effector genes are indicated by colored boxes according to their candidate effector family (Müller et al. 2019).**
340 **Grey boxes indicate non-effector genes. Loci were manually checked and low-confidence genes (i.e. pseudogenes,**
341 **transposable elements) were removed. Asterisks in panel E) indicate small inversions affecting a candidate effector**
342 **gene.**

343



344

345 **Fig. 4 Analysis of avirulence genes in *B.g. triticales* THUN-12.** **A)** Summary of gene expression of all
 346 genes in isolate THUN-12 at two days post infection (2dpi) on susceptible triticales cultivar ‘Timbo’.
 347 Gene expression is displayed as log₂-transformed TPM values. Values for avirulence genes are indicated
 348 as black dots. There are several gene copies of *AvrPm17* and *AvrPm3^{a2/f2}* in the THUN-12 genome.
 349 *AvrPm17* gene copies differ by two SNPs and are represented separately. Two of the *AvrPm3^{a2/f2}* copies
 350 are identical and represented (v1,v2) as a single data point, whereas the third copy carries a single
 351 synonymous SNP (v3) and is represented separately **B)** phenotypes of isolate THUN-12 at 10dpi on
 352 wheat differential lines or transgenic lines containing *Pm17* in the ‘Bobwhite’ background **C)** Result of
 353 the single interval QTL mapping approach, based on 55 randomly selected progeny of the mapping
 354 population Bgt_96224 X THUN-12 on the *Pm3c* containing NIL Sonora/8*CC. The black line indicates
 355 the logarithm of the odd score (LOD score) of the association. The dashed red line indicates the
 356 significance threshold estimated by 1000 permutations. **D)** represents the region corresponding to the
 357 1.5LOD interval in the two genomes of isolates Bgt_96224 and THUN-12. Genes are indicated by
 358 colored boxes. Gene orientation is indicated by arrows. Members of different candidate effector families
 359 are represented by different colors as indicated.

360